


## ORIGINAL ARTICLE OPEN ACCESS

# Mitigating Ibrutinib-Induced Ventricular Arrhythmia and Cardiac Dysfunction With Metformin

Pengsha Li<sup>1</sup> | Daiqi Liu<sup>1</sup> | Pan Gao<sup>1</sup>  | Ming Yuan<sup>1,2</sup> | Zhiqiang Zhao<sup>1</sup> | Yue Zhang<sup>1</sup> | Zandong Zhou<sup>1</sup> | Qingling Zhang<sup>1</sup> | Meng Yuan<sup>1</sup> | Xing Liu<sup>1</sup> | Gary Tse<sup>1,3</sup> | Guangping Li<sup>1</sup> | Qiankun Bao<sup>1</sup> | Tong Liu<sup>1</sup>

<sup>1</sup>Tianjin Key Laboratory of Ionic-Molecular Function of Cardiovascular Disease, Department of Cardiology, Tianjin Institute of Cardiology, Second Hospital of Tianjin Medical University, Tianjin, China | <sup>2</sup>Key Laboratory of Cardiovascular Intervention and Regenerative Medicine of Zhejiang Province, Department of Cardiology, Sir Run Run Shaw Hospital, Zhejiang University School of Medicine, Hangzhou, China | <sup>3</sup>Kent and Medway Medical School, Canterbury, UK

**Correspondence:** Tong Liu ([liutong@tmu.edu.cn](mailto:liutong@tmu.edu.cn); [liutongdoc@126.com](mailto:liutongdoc@126.com))

**Received:** 5 February 2024 | **Revised:** 24 May 2024 | **Accepted:** 6 June 2024

**Funding:** National Natural Science Foundation of China (Grants: 82170327, 82200344, 82370332); Tianjin Key Medical Discipline (Specialty) Construction Project (Grant: TJYXZDXK-029A); Tianjin Natural Science Foundation (Grants: 20JCZDJC00340, 20JCZXJC00130).

**Keywords:** Ibrutinib | metformin | PI3K-AKT pathway | ventricular arrhythmia

## ABSTRACT

**Background:** Ibrutinib is a first-line drug that targets Bruton's tyrosine kinase for the treatment of B cell cancer. However, cardiotoxicity induced by ibrutinib is a major side effect that limits its clinical use. This study aimed to investigate the mechanism of ibrutinib-induced cardiotoxicity and evaluate the protective role of metformin.

**Methods:** The study utilized male C57BL/6J mice, which were administered ibrutinib at a dosage of 30 mg/kg/day via oral gavage for 4 weeks to induce cardiotoxicity. Metformin was administered orally at 200 mg/kg/day for 5 weeks, starting 1 week before ibrutinib treatment. Cardiac function was assessed using echocardiography and electrophysiological studies, including surface electrocardiography and epicardial electrical mapping. Blood pressure was measured using a tail-cuff system. Western blot analysis was conducted to evaluate the activity of the PI3K-AKT and AMPK pathways, along with apoptosis markers.

**Results:** C57BL/6J mice were treated with ibrutinib for 4 weeks to assess its effect on cardiac function. We observed that ibrutinib induced ventricular arrhythmia and abnormal conduction while reducing the left ventricular ejection fraction. Furthermore, pretreatment with metformin reversed ibrutinib-induced cardiotoxicity. Mechanistically, ibrutinib decreased PI3K-AKT activity, resulting in apoptosis of cardiomyocytes. Administration of metformin upregulated AMPK and PI3K-AKT activity, which contributed to the improvement of cardiac function.

**Conclusion:** The study concludes that metformin effectively mitigates ibrutinib-induced cardiotoxicity, including ventricular arrhythmia and cardiac dysfunction, by enhancing AMPK and PI3K-AKT pathway activity. These findings suggest that metformin holds potential as a therapeutic strategy to protect against the adverse cardiac effects associated with ibrutinib treatment, offering a promising approach for improving the cardiovascular safety of patients undergoing therapy for B cell cancers.

**Abbreviations:** AMPK, AMP-activated protein kinase; BTK, Bruton's tyrosine kinase; CV, conduction velocity; DBP, diastolic blood pressure; IVS, interventricular septal thickness; LV, left ventricle; LVEDD, left ventricular end-diastolic dimension; LVEF, left ventricular ejection fraction; LVESD, left ventricular end-systolic dimension; LVFS, left ventricular fractional shortening; LVPW, left ventricular posterior wall thickness; MBP, mean blood pressure; PI3K, phosphatidylinositol 3-kinase; QTC, corrected QT interval; RV, right ventricle; SBP, systolic blood pressure; SEM, standard error of the mean.

Pengsha Li, Daiqi Liu, and Pan Gao contributed equally to this work and shared the co-first authorship.

This is an open access article under the terms of the [Creative Commons Attribution-NonCommercial](https://creativecommons.org/licenses/by-nc/4.0/) License, which permits use, distribution and reproduction in any medium, provided the original work is properly cited and is not used for commercial purposes.

© 2025 The Author(s). *Cancer Innovation* published by John Wiley & Sons Ltd on behalf of Tsinghua University Press.

## 1 | Introduction

Ibrutinib, which is an oral Bruton's tyrosine kinase (BTK) inhibitor, is approved for the treatment of chronic lymphocytic leukemia, mantle cell lymphoma, Waldenström macroglobulinemia, and marginal cell lymphoma by the US Food and Drug Administration [1, 2]. Ibrutinib can improve survival and overall tolerability compared with traditional systemic chemotherapy. However, patients who use ibrutinib experience an increased incidence of ventricular and atrial arrhythmias, conduction disorders, heart failure [3], hypertension [4], and other cardiovascular events [5–8]. Ventricular arrhythmias, such as frequent premature ventricular contractions and ventricular tachycardia, increase the risk of sudden cardiac death [7]. Recurrent polymorphic ventricular tachycardia and sudden death have been consistently associated with the administration of ibrutinib [9]. Therefore, determining the mechanisms underlying ibrutinib-induced ventricular arrhythmia and developing novel therapeutic strategies are urgently required.

Multiple mechanisms regarding the pathogenesis of ibrutinib-induced arrhythmia, involving on-target and off-target effects because ibrutinib inhibits at least 19 kinases including BTK, have been reported [10]. Upon antigen binding, BTK can be phosphorylated by the upstream tyrosine-protein kinase Syk or Lyn, resulting in the activation of downstream nuclear factor- $\kappa$ B and phosphatidylinositol 3-kinase (PI3K) cascades [10, 11]. Activation of PI3K (p110 $\alpha$ ) is a major regulator in maintaining sinus rhythm, and ibrutinib decreases PI3K-AKT activity in neonatal rat ventricular myocytes [12, 13]. These findings suggest the involvement of the PI3K-AKT pathway in ibrutinib-induced ventricular arrhythmia. AMP-activated protein kinase (AMPK), which is a stress kinase that functions as an energy sensor and monitors the ATP/ADP ratio, is responsible for AKT phosphorylation independent of PI3K [14]. Metformin is an oral medication used to lower high blood sugar concentrations in patients with type 2 diabetes since its introduction in 1957 [15]. Metformin is believed to primarily exert its antidiabetic effects by suppressing hepatic glucose production and activating AMPK [16]. Recent research has shown that metformin exerts a beneficial effect on cardiovascular protection, resulting in a considerable improvement in left ventricular function and survival through the activation of AMPK [17–20]. Metformin also reduces cardiovascular disease risk factors, such as blood lipids, body weight, and blood pressure. Metformin decreases the risk of all-cause mortality and the incidence of cardiovascular disease compared with insulin and other oral hypoglycemic medications [21, 22]. Studies have shown that patients with diabetes who are treated with metformin have a lower incidence of cancer. The antitumor effects of metformin are closely associated with the mechanistic target of rapamycin (mTOR) complex 1, which is a key protein in the PI3K/Akt/mTOR pathway [23–25]. Therefore, we hypothesize that metformin can reduce ibrutinib-induced cardiotoxicity.

In the present study, we established a model of ibrutinib-induced ventricular arrhythmia and investigated its underlying mechanism. This study showed that ibrutinib decreased PI3K-AKT activity in the ventricles. Additionally, metformin attenuated ibrutinib-induced cardiotoxicity by increasing the activity of AMPK and PI3K-AKT, indicating the potential combination of metformin and ibrutinib as a therapeutic approach for B cell cancer.

## 2 | Materials and Methods

### 2.1 | Experimental Protocol

Male C57BL/6J mice aged 3 months were treated with ibrutinib (30 mg/kg/day) via oral gavage for 4 weeks [1]. Mice in the control group were administered the equivalent amount of solvent. Metformin was administered orally at 200 mg/kg/day for 5 weeks, starting 1 week before initiating ibrutinib treatment [26]. The metformin group received metformin alone for 5 weeks using the same administration method. Ibrutinib and metformin were purchased from MedChemExpress (Cat No. PCI-32765) and Sigma-Aldrich (Cat No. PHR1084), respectively. Animal protocols received approval from the Experimental Animal Administration Committee of Tianjin Medical University (TMUaMEC 2019004).

### 2.2 | Blood Pressure Measurement

Blood pressure of the mice was monitored using a tail-cuff system (Softron TMC-213). When the wave was sinusoidal, the following indices were recorded: heart rate, systolic blood pressure (SBP), diastolic blood pressure (DBP), and mean blood pressure (MBP).

### 2.3 | Echocardiographic Assessments

After the treatment period, the mice were weighed and anesthetized with the inhalation of isoflurane. Transthoracic echocardiography was performed using a small animal ultrasound system (Visual Sonics Vevo 2100). Echocardiographic parameters were acquired in the short-axis and long-axis views and measured using M-mode imaging during three consecutive cardiac ejection cycles.

### 2.4 | Electrophysiology Study

After anesthetization, the mice were positioned on their backs on a surgical table. A standard lead II body surface electrocardiogram was recorded before the operation. The jugular vein was exposed under a dissecting microscope and the distal end was ligated. A 1.1 F octapolar electrophysiological catheter was inserted and advanced through the right atrium to the right ventricle (RV) [27–29]. The catheter positioning was monitored and located using a body surface electrocardiogram. Ventricular arrhythmia was induced by a standard burst pacing protocol. The RR interval and the QT interval were measured using LabChart8 Pro.

### 2.5 | Epicardial Electrical Mapping

Ventricular electrical conduction heterogeneity and ventricular tachycardia induction rates were assessed using an electrical mapping system, as described in a previous study [30]. Briefly, after an electrophysiological study, a 0.5-inch incision was made on the right side of the midline at the level of the clavicle. A blunt dissection was performed to separate the subcutaneous tissue, thyroid, and lymph tissue and isolate the neck trachea. A 6/0 thread was placed below the trachea and an incision was created using micro-scissors. Ventilator parameters were set

with a respiration frequency of 110 Hz, a respiration ratio of 1:1, and a tidal volume of 1.0 mL. The ventilator for mechanical ventilation was connected and tracheal intubation was secured with sutures. The skin of the lower abdomen was cut below the xiphoid process to expose the abdominal organs. The diaphragm was opened and the heart was then exposed. We used 6×6 microelectrodes to record the epicardial activation map of the left ventricle (LV) and RV. Data were recorded using a multichannel system (EMS64-USB-1003). Conduction velocity, absolute inhomogeneity, and the inhomogeneity index were calculated using EMapScope 4.0 software (MappingLab Ltd.).

## 2.6 | Western Blot Analysis

Total protein from frozen ventricular tissue was extracted using radioimmunoprecipitation assay lysis buffer. The protein concentration in the supernatant was determined using the bicinchoninic acid method. We used polyacrylamide gel electrophoresis for western blot analysis. Protein samples (30 µg) were transferred to a solid-phase carrier (polyvinylidene fluoride membrane) after separation using polyacrylamide gel electrophoresis. The protein on the solid-phase carrier served as the antigen and reacted with the corresponding antibody. The antibody then reacted with the horseradish peroxidase-linked second antibody. After substrate color development, this process allowed for the detection of protein components expressed by the specific target gene that were separated by electrophoresis. The following antibodies were used: glyceraldehyde-3-phosphate dehydrogenase (1:5000; Proteintech), phosphorylated-AMPK $\alpha^{\text{Thr172}}$  ([p-AMPK $\alpha^{\text{Thr172}}$ ] 1:1000, 2535S; Cell Signaling Technology), total-AMPK $\alpha$  ([t-AMPK] 1:1000, ab32047; Abcam), PI3K (p110 $\alpha$ ) (1:1000, 4249S; Cell Signaling Technology), total-AKT ([t-AKT] 1:1000, 4685S; Cell Signaling Technology), phosphorylated-AKT $\text{Ser473}$  ([p-AKT $\text{Ser473}$ ] 1:1000, 4060S; Cell Signaling Technology), Bcl-2 (1:1000, ab59348; Abcam), Bax (1:5000, ab32503; Abcam), and  $\alpha$ -smooth muscle actin ([ $\alpha$ -SMA] 1:1000, 19245S; Cell Signaling Technology).

## 2.7 | Histological Analysis

Mouse ventricular tissue samples were dehydrated using an automatic dehydrator. After the dehydration process, they were transferred to liquified paraffin for embedding. Once the paraffin was fully solidified, the wax block was sectioned continuously (5 µm). The slides were placed in a constant temperature water bath, and each section was quickly transferred onto a glass slide. The slides were baked in a 65°C oven for 60 min and then stored at room temperature. Hematoxylin and eosin staining and Masson staining were performed to observe the morphology and assess fibrosis in the LV. Images were captured using an Olympus microscope. The extent of interstitial fibrosis was quantified in each of the five random fields in each section using ImageJ software (Bethesda).

## 2.8 | Statistical Analysis

Measurement data are expressed as the mean  $\pm$  standard error of the mean (SEM). Before applying statistical methods, we

evaluated whether the data fit a normal distribution by conducting the Shapiro–Wilk test, and a  $p > 0.05$  was considered to follow a normal distribution. Levene's test was used to test the homogeneity of variance for two independent samples.  $p > 0.05$  indicated that the variance was homogeneous using the  $t$ -test, and  $p \leq 0.05$  indicated that the variance was not homogeneous using Welch's  $t$ -test. Similarly, a  $p > 0.05$  in one-way analysis of variance suggested homogeneity of variance, whereas a  $p \leq 0.05$  in the Welch analysis of variance indicated a lack of homogeneity for three or more samples. Nonparametric data were analyzed with the Mann–Whitney or Kruskal–Wallis test. Data were statistically analyzed using SPSS 26.0 software. A  $p < 0.05$  was considered statistically significant.

## 3 | Results

### 3.1 | Ibrutinib Promotes Electrical Remodeling

A model of ibrutinib-induced cardiotoxicity using C57BL/6J mice was established (Figure 1a). Ibrutinib-treated mice showed prolongation of the corrected QT interval (QTc), but not of the RR interval (Figure 1b,c). Furthermore, we recorded electrical conduction mapping of the LV and RV in vivo. Conduction velocity was decreased and conduction heterogeneity was increased in the LV and RV of ibrutinib-treated mice, with increased absolute inhomogeneity and an increased inhomogeneity index (Figure 1d–j). These results suggest that ibrutinib causes electrical remodeling.

### 3.2 | Ibrutinib Induces Cardiac Dysfunction and Ventricular Structural Remodeling

We next examined the effect of ibrutinib on blood pressure and cardiac function. Ibrutinib-treated mice showed a significant reduction in the left ventricular ejection fraction ( $p = 0.0322$ ) and left ventricular fractional shortening ( $p = 0.0355$ ) when compared to control mice (Figure 2a–c). Interventricular septal thickness, left ventricular posterior wall thickness, and E/e' showed a downward trend and the left ventricular end-diastolic dimension and the left ventricular end-systolic dimension showed an increasing trend in ibrutinib-treated mice when compared to control mice (Table 1). In addition, ibrutinib treatment increased SBP and DBP (Figure 2d). Moreover, ibrutinib-treated mice showed greater deposition of collagen fibers in the ventricular interstitium (Figure 2e,f), accompanied by higher  $\alpha$ -SMA expression in the ventricles than control mice (Figure 2g,h). These findings suggest that ibrutinib induces ventricular structural remodeling.

### 3.3 | Ibrutinib Reduces PI3K-AKT Pathway Activity

To determine the mechanism of ibrutinib-induced cardiotoxicity, we performed western blot analysis to detect PI3K-AKT pathway activity. PI3K (p110 $\alpha$ ) and p-AKT $\text{Ser473}$  protein levels were lower in the ventricles of ibrutinib-treated mice than in control mice (Figure 3a–c). The PI3K-AKT pathway plays a

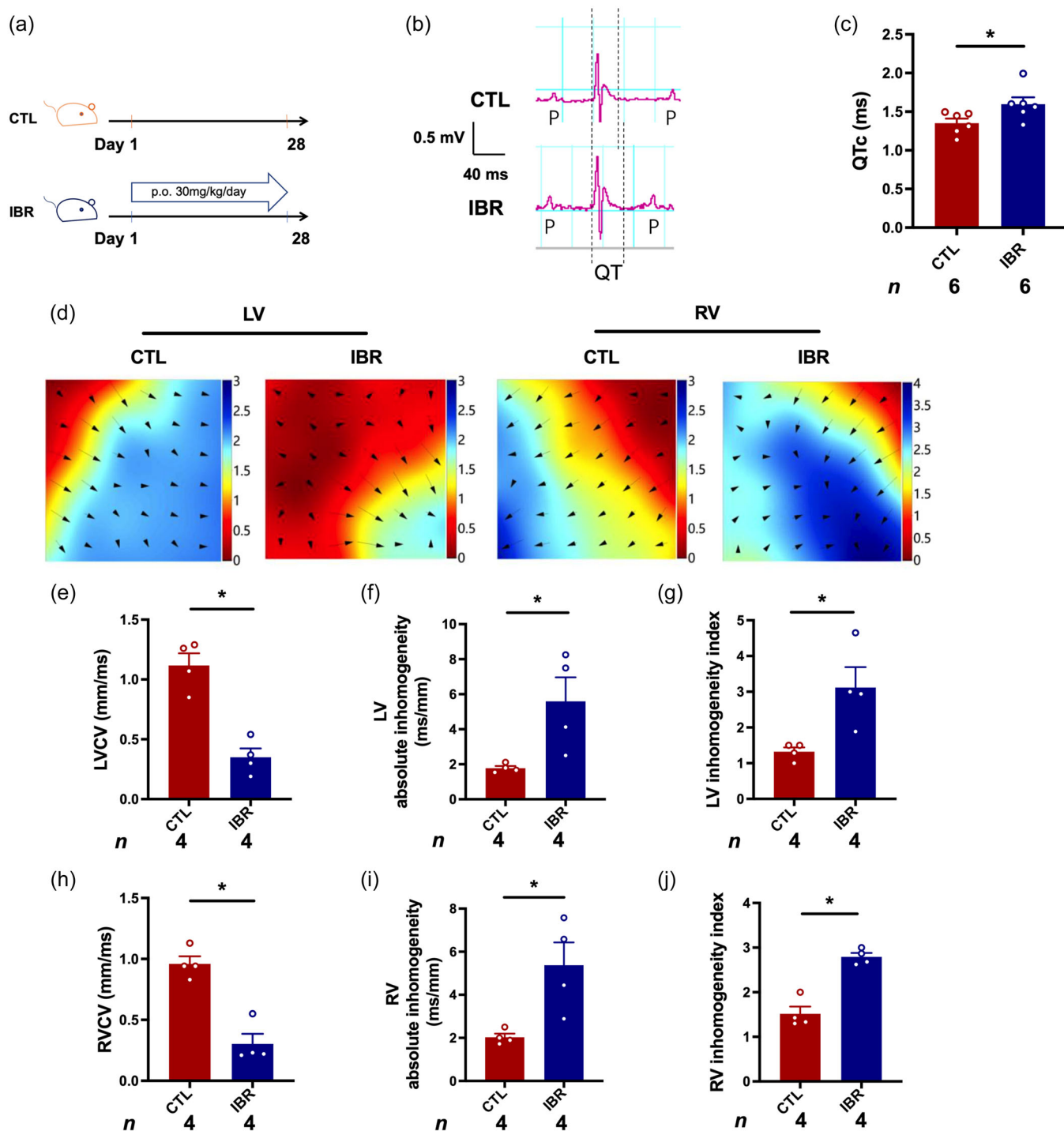


**FIGURE 1** | Ibrutinib promotes ventricular arrhythmia and electrical remodeling. (a) C57BL/6J mice were treated with ibrutinib (IBR) at 30 mg/kg/day or vehicle (control [CTL]) for 28 days. (b) Representative electrocardiographic tracings for control and ibrutinib-treated mice. (c) Corrected QT interval (QTc). Data are the mean  $\pm$  SEM,  $n = 6$  in each group;  $*p < 0.05$ , Student's  $t$ -test. (d) Representative epicardial electrical mapping of the left ventricle (LV) and right ventricle (RV) in vivo. (e–j) Conduction velocity (CV) of the LV (e) and RV (h), absolute inhomogeneity of the LV (f) and RV (i), and the inhomogeneity index of the LV (g) and RV (j) were measured. Data are the mean  $\pm$  SEM,  $n = 4$  in each group;  $*p < 0.05$ , Student's  $t$ -test.

predominant role in antiapoptotic effects in the cardiovascular system [31, 32]. Therefore, we examined the cell apoptosis markers Bax and Bcl-2. The ratio of Bax/Bcl-2 was higher in ibrutinib-treated mice than in control mice (Figure 3a,e). This finding suggests that ibrutinib promotes cardiomyocyte apoptosis via downregulation of PI3K-AKT pathway activation, leading to cardiotoxicity.

### 3.4 | Metformin Improves Ibrutinib-Induced Ventricular Arrhythmia

Metformin is the first-line drug for the treatment of type 2 diabetes mellitus and is associated with few adverse cardiovascular events in clinical trials and observational studies [33, 34]. To investigate the effect of metformin on



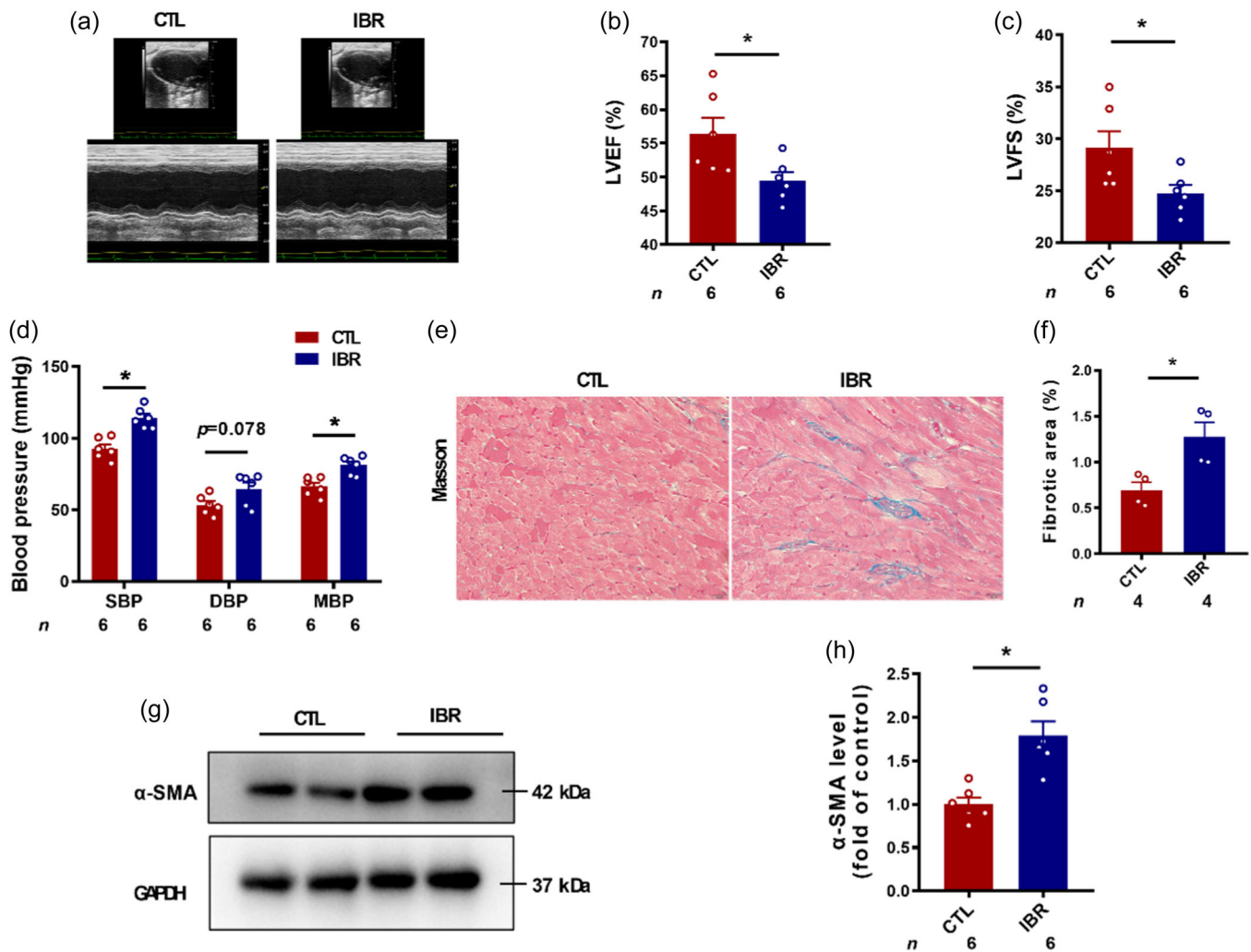


**FIGURE 2** | Ibrutinib induces cardiac dysfunction and ventricular structural remodeling. C57BL/6J mice were treated with ibrutinib (IBR) at 30 mg/kg/day or vehicle (control [CTL]) for 28 days. (a) Representative two-dimensional and M-mode views of the left ventricle (LV). (b) The left ventricular ejection fraction (LVEF) and (c) left ventricular fractional shortening (LVFS) were measured. Data are the mean  $\pm$  SEM,  $n = 6$  in each group;  $*p < 0.05$ , Student's  $t$ -test. (d) Systolic blood pressure (SBP), diastolic blood pressure (DBP), and mean blood pressure (MBP) were measured after treatment. Data are the mean  $\pm$  SEM,  $n = 6$  in each group;  $*p < 0.05$ , Student's  $t$ -test for SBP and MBP, and DBP was analyzed using the Mann-Whitney test. (e) Representative images of Masson staining of ventricular tissue in the two groups. (f) Quantification of the fibrotic area shown in panel (e). Data are the mean  $\pm$  SEM,  $n = 4$  in each group;  $*p < 0.05$ , Student's  $t$ -test. (g, h) Protein expression and quantification of  $\alpha$ -smooth muscle actin ( $\alpha$ -SMA) in the LV. Data are the mean  $\pm$  SEM,  $n = 6$  in the CTL group and  $n = 6$  in the IBR group;  $*p < 0.05$ , Student's  $t$ -test.

**TABLE 1** | Echocardiographic characteristics of mice in the CTL and IBR groups.

Parameters	CTL	IBR
LVEF (%)	$55.53 \pm 2.46$	$47.70 \pm 1.14^*$
LVFS (%)	$28.55 \pm 1.60$	$23.63 \pm 0.73^*$
IVS (mm)	$0.87 \pm 0.05$	$0.75 \pm 0.10$
LVEDD (mm)	$3.83 \pm 0.07$	$3.93 \pm 0.14$
LVEDS (mm)	$2.62 \pm 0.15$	$2.90 \pm 0.15$
LVPW (mm)	$0.88 \pm 0.05$	$0.73 \pm 0.08$
E/e'	$1.66 \pm 0.19$	$1.48 \pm 0.06$

Note: Values are expressed as the mean  $\pm$  SEM.  $n = 6$  mice in each group. CTL refers to the control group, and IBR refers to the ibrutinib group.

$*p < 0.05$  versus the CTL group. Data were analyzed by Student's  $t$ -test.

ibrutinib-induced cardiotoxicity, we administered metformin (200 mg/kg/day) 1 week before ibrutinib treatment and metformin alone for 5 weeks (Figure 4a). A surface electrocardiogram and intracardiac electrogram showed the development of ventricular premature contractions after burst stimulation in ibrutinib-treated mice (Figure 4b). In contrast, burst pacing stimulation failed to induce any ventricular arrhythmias in control mice. Metformin shortened the prolonged QTc induced by ibrutinib (Figure 4c,d). Moreover, metformin reversed the decreased conduction velocity by ibrutinib and reversed the increased absolute heterogeneity and heterogeneity index by ibrutinib in the LV and RV (Figure 4e-k). These results suggest that metformin ameliorates ibrutinib-induced ventricular arrhythmia and electrical remodeling.

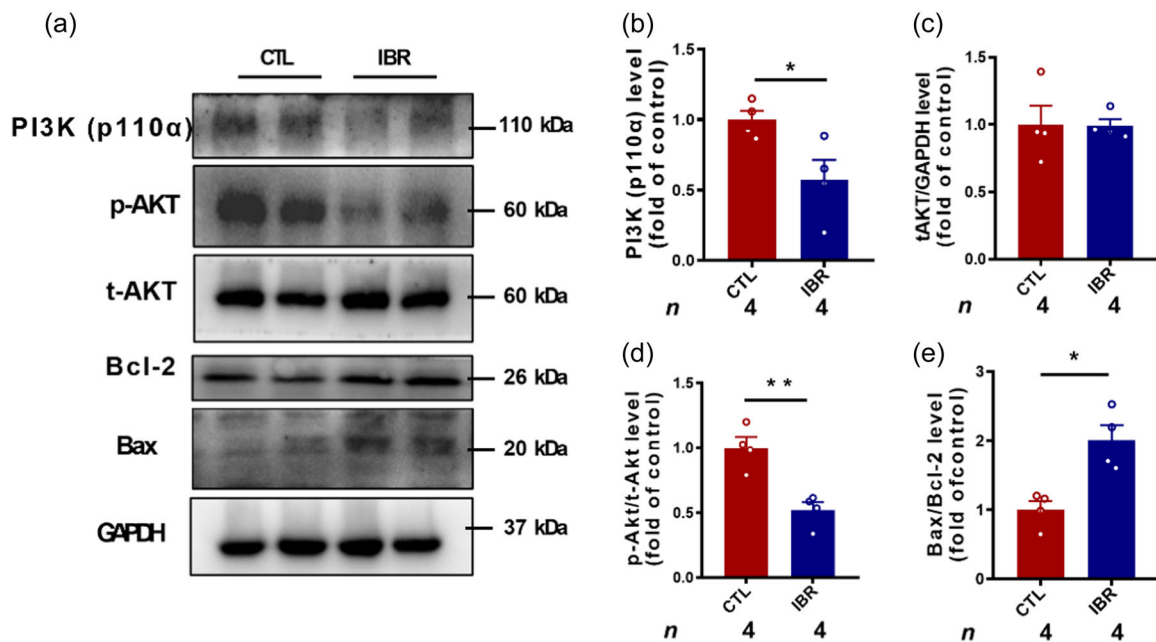


**FIGURE 3** | Ibrutinib reduces PI3K-AKT pathway activity. C57BL/6 J mice were treated with ibrutinib (IBR) at 30 mg/kg/day or vehicle (control [CTL]) for 28 days. (a) Protein expression of PI3K (p110α), p-AKT<sup>Ser473</sup>, t-AKT, Bcl-2, Bax, and GAPDH in the ventricles in the two groups. (b–e) Quantification of PI3K (p110α), p-AKT<sup>Ser473</sup>/t-AKT, t-AKT, and Bax/Bcl-2. Data are the mean ± SEM, *n* = 4 in each group; \**p* < 0.05, \*\**p* < 0.01; Student's *t*-test.

### 3.5 | Metformin Attenuates Ibrutinib-Induced Cardiac Dysfunction and Ventricular Structural Remodeling

We detected blood pressure and cardiac function after metformin treatment. Echocardiographic analysis showed that metformin pretreatment rescued the ibrutinib-mediated reduction in the left ventricular ejection fraction and left ventricular fractional shortening (Figure 5a–c). Metformin reversed the decrease in the interventricular septal thickness, left ventricular posterior wall thickness, and E/e by ibrutinib treatment and reduced the increase in the left ventricular end-diastolic dimension and left ventricular end-systolic dimension by ibrutinib treatment (Table 2). Moreover, metformin reduced the increase in SBP and DBP caused by ibrutinib treatment (Figure 5d). In a pathological analysis, metformin treatment reduced the increase in deposition of collagen fibers in the ventricular interstitium caused by ibrutinib treatment (Figure 5g,h). Consistently, metformin reversed the upregulated α-SMA expression by ibrutinib treatment in the ventricles (Figure 5e,f), suggesting that metformin ameliorates ibrutinib-induced ventricular structural remodeling.

### 3.6 | Metformin Promotes AMPK and PI3K-AKT Pathway Activity

Metformin is an established agonist of AMPK, which inhibits the activity of mitochondrial complex I [35]. To further study the mechanisms underlying the protective effect of metformin in ibrutinib-induced cardiotoxicity, we investigated the signaling molecules in the AMPK and PI3K-AKT pathways. Western blot results showed that metformin treatment reversed the decrease in levels of PI3K (p110α), p-AKT<sup>Ser473</sup>, and

AMPK<sup>Thr172</sup> caused by ibrutinib treatment (Figure 6a–c,e). In addition, metformin treatment reduced the increase in the Bax/Bcl-2 ratio caused by ibrutinib treatment (Figure 6g), suggesting that metformin improves apoptosis of cardiomyocytes.

## 4 | Discussion

Ibrutinib, which is an oral BTK inhibitor, considerably improves the prognosis of various B cell malignant diseases and is approved for lifelong therapy. However, ibrutinib has been associated with a more than six-fold increase in the incidence of cardiac arrhythmias, including atrial fibrillation and potentially fatal ventricular arrhythmic episodes [36, 37]. Atrial fibrillation is the leading cause of drug discontinuation in patients receiving ibrutinib owing to toxicity concerns. Atrial fibrillation occurs in 5%–16% of patients, particularly in those aged 65 years or older and/or with cardiovascular risk factors [38]. Ibrutinib is also associated with an increase in ventricular arrhythmic events and sudden cardiac deaths. In cohort studies, the incidence of ventricular arrhythmic events and sudden cardiac deaths ranged from 195 to 1453/100,000 person-years. The risk of ventricular tachycardia or sudden cardiac death in the general population of 65-year-old people ranges from 200 to 400 events/100,000 person-years [38]. To examine the arrhythmogenic mechanisms that contribute to this outcome, we attempted to establish a mouse model that closely mimics the clinical characteristics of affected patients. The therapeutic effect of ibrutinib is dose-dependent. In one study, esophageal stimulation-induced atrial fibrillation was associated with an increase in oxidative stress signaling after 14 days of ibrutinib 30 mg/kg/day [1]. Therefore, we used 30 mg/kg/day as the ibrutinib dose in the present study. We found that ibrutinib impaired ventricular conduction and increased conduction

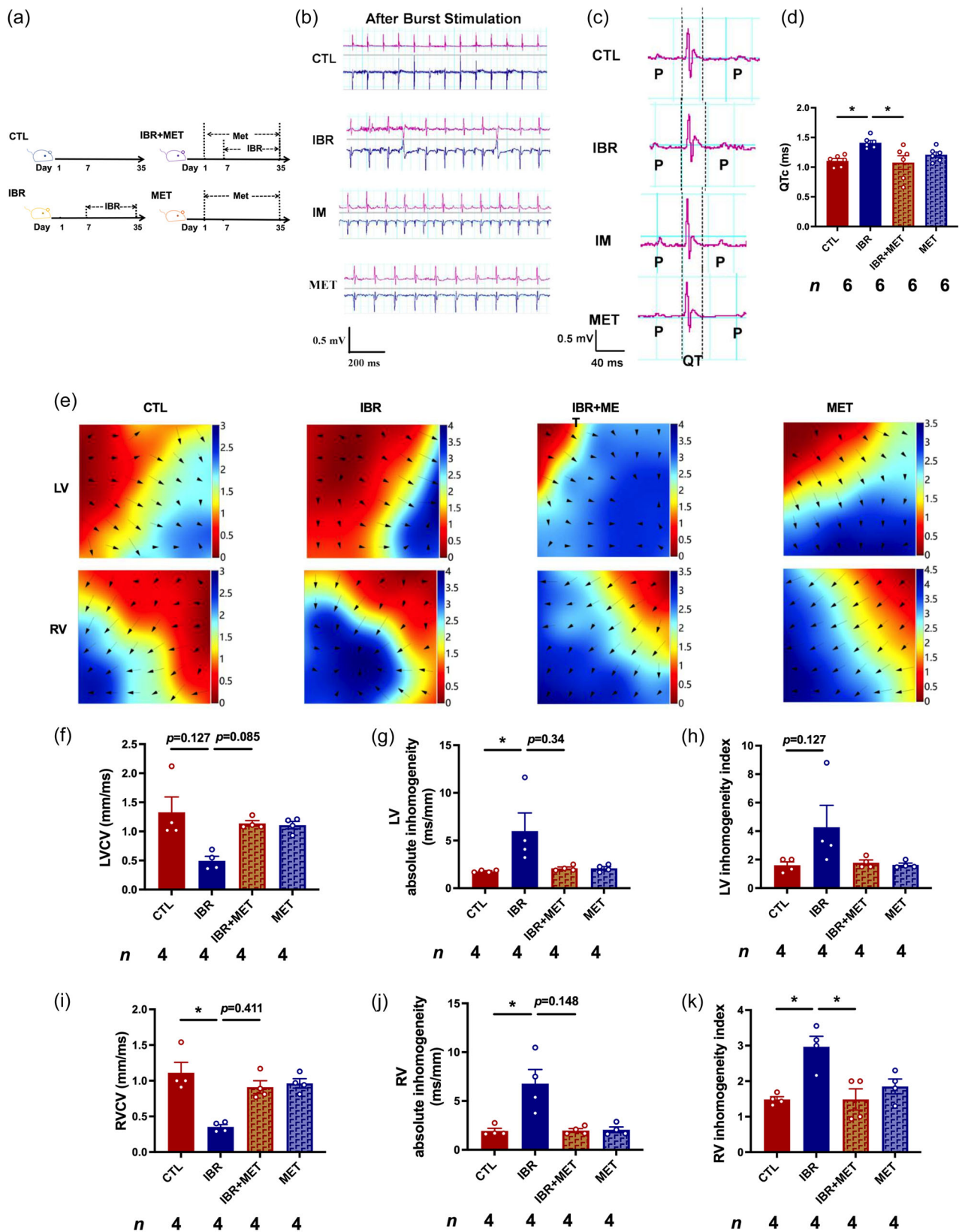


**FIGURE 4** | Metformin improves ibrutinib-induced ventricular arrhythmia. (a) Mice that received ibrutinib (IBR) or vehicle treatment were administered metformin (MET) at 200 mg/kg/day. (b) Representative surface electrocardiography in the four groups. (c) Representative electrocardiographic tracings of mice in the four groups. (d) Corrected QT interval (QTc). Data are the mean  $\pm$  SEM,  $n = 6$  in each group; \* $p < 0.05$ , one-way ANOVA with Tukey's multiple comparison test. (e) Representative epicardial electrical mapping of the left ventricle (LV) and right ventricle (RV) of mice in the four groups. (f-k) Conduction velocity (CV) of the LV (f) and the RV (i), absolute inhomogeneity of the LV (g) and the RV (j), and the inhomogeneity index of the LV (h) and the RV (k) were measured. Data are the mean  $\pm$  SEM,  $n = 4$  in each group; \* $p < 0.05$ , Kruskal-Wallis test.

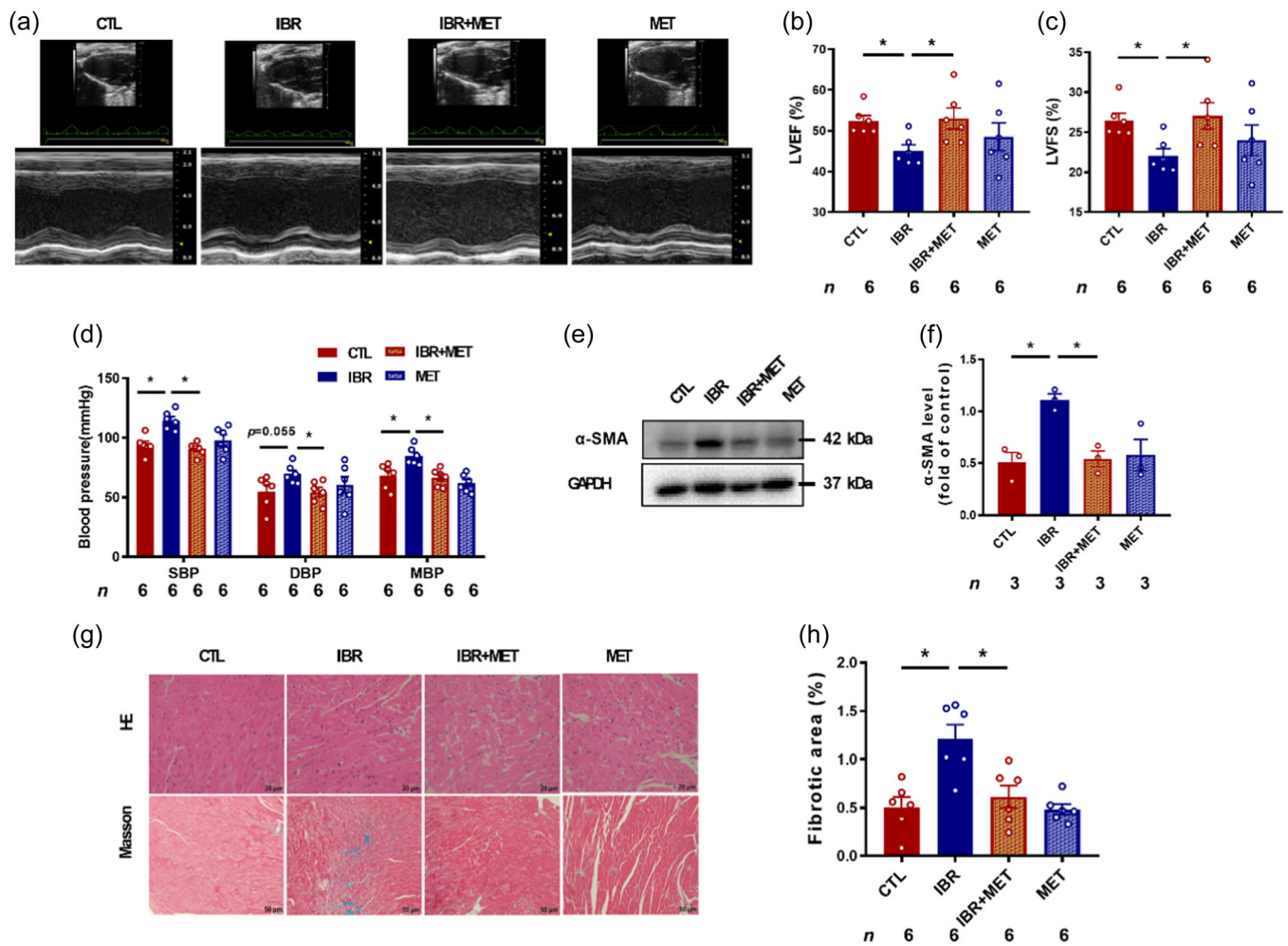


**FIGURE 5** | Metformin attenuates ibrutinib-induced cardiac dysfunction and ventricular structural remodeling. Mice that received ibrutinib (IBR) or vehicle treatment were administered metformin (MET) at 200 mg/kg/day. (a) Representative two-dimensional and M-mode views of the left ventricle (LV). (b,c) The left ventricular ejection fraction (LVEF) and left ventricular fractional shortening (LVFS) were measured. Data are the mean ± SEM,  $n = 6$  in each group;  $*p < 0.05$ , one-way analysis of variance with Tukey's multiple comparison test. (d) Systolic blood pressure (SBP), diastolic blood pressure (DBP), and mean blood pressure (MBP) were measured after treatment. Data are the mean ± SEM,  $n = 6$  in each group;  $*p < 0.05$ , one-way analysis of variance with Tukey's multiple comparison test. (e, f) Protein expression and quantification of  $\alpha$ -SMA in the LV. Data are the mean ± SEM,  $n = 3$  in each group;  $*p < 0.05$ , one-way analysis of variance with Tukey's multiple comparison test. (g) Representative images of hematoxylin and eosin staining (scale bar = 20  $\mu$ m) and Masson staining (scale bar = 50  $\mu$ m) of the LV. (h) Quantification of the fibrotic area shown in panel (g). Data are the mean ± SEM,  $n = 6$  in each group;  $*p < 0.05$ , one-way analysis of variance with Tukey's multiple comparison test.

**TABLE 2** | Echocardiographic characteristics of mice in the four groups.

Parameters	CTL	IBR	IBR + MET	MET
LVEF (%)	55.22 ± 1.64	45.14 ± 1.45*	53.00 ± 2.56 <sup>#</sup>	48.52 ± 3.39
LVFS (%)	28.37 ± 1.11	22.09 ± 0.86*	27.02 ± 1.67 <sup>#</sup>	23.98 ± 1.89
IVS (mm)	0.89 ± 0.06	0.80 ± 0.04	0.81 ± 0.03	0.70 ± 0.03
LVEDD (mm)	3.93 ± 0.14	3.99 ± 0.12	3.95 ± 0.11	3.82 ± 0.16
LVESD (mm)	2.78 ± 0.13	3.07 ± 0.11	2.86 ± 0.09	2.82 ± 0.19
LVPW (mm)	0.96 ± 0.04	0.88 ± 0.05	0.89 ± 0.04	0.80 ± 0.03
E/e'	1.66 ± 0.21	1.29 ± 0.05	1.45 ± 0.13	1.46 ± 0.16

Note: Values are expressed as the mean ± SEM.  $n = 6$  mice in each group.

Abbreviations: IBR, ibrutinib; IVS, interventricular septal; LVEDD, left ventricular end-diastolic dimension; LVEF, left ventricular ejection fraction; LVESD, left ventricular end-systolic dimension; LVFS, left ventricular fractional shortening; LVPW, left ventricular posterior wall; MET, metformin.

\* $p < 0.05$  vs the CTL group.

<sup>#</sup> $p < 0.05$  vs the IBR group, one-way analysis of variance with Tukey's post hoc test.



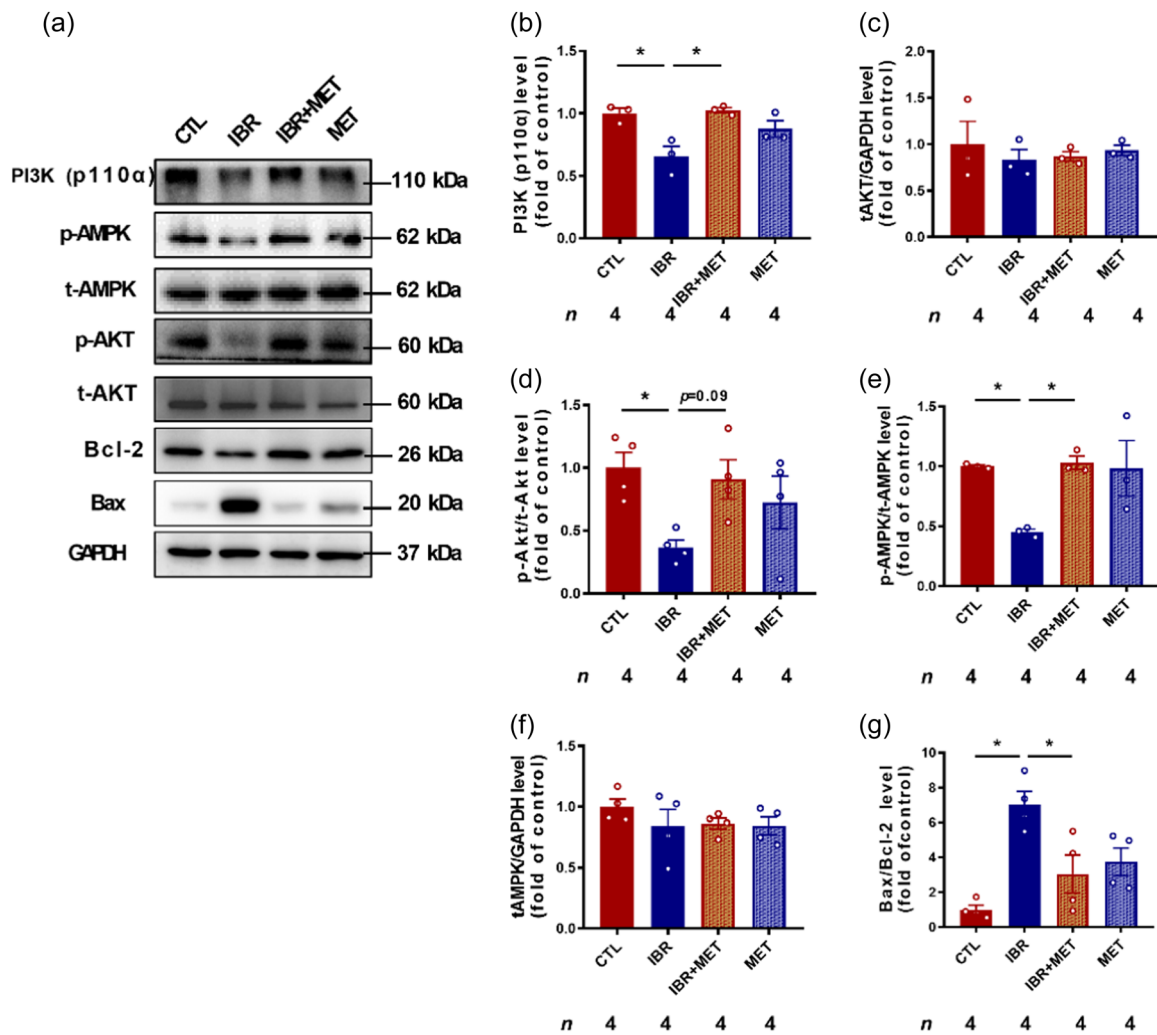


**FIGURE 6** | Metformin promotes AMPK and PI3K-AKT pathway activity. Mice that received ibrutinib (IBR) or vehicle treatment were administered metformin (MET) at 200 mg/kg/day. (a) Protein expression of PI3K(p110α), p-AMPK, t-AMPK, p-AKT<sup>Ser473</sup>, t-AKT, Bcl-2, Bax, and GAPDH in the ventricles. (b–g) Quantification of PI3K (p110α), p-AMPK/t-AMPK, t-AMPK, p-AKT<sup>Ser473</sup>/t-AKT, t-AKT, and Bax/Bcl-2 shown in panel (a). Data are the mean ± SEM, *n* = 4 in each group; \**p* < 0.05, one-way analysis of variance with Tukey's multiple comparison test and Student's *t*-test.

heterogeneity. The QT interval represents the sum of the ventricular depolarization and repolarization potential times. QTc prolongation is often a predictor of the ventricular arrhythmic risk and sudden cardiac death, and it is commonly corrected using Bazett's formula [39]. QTc prolongation is a common cardiac finding following tyrosine kinase inhibitor treatment [40]. In our study, we observed a prolonged QTc interval following ibrutinib treatment, which was associated with the development of ventricular premature contractions. Furthermore, studies have shown that ibrutinib treatment alters cardiac ion channel currents, including K<sup>+</sup> and Na<sup>+</sup> currents [5]. Our analysis showed abnormalities in conduction and repolarization, which could potentially be explained by altered cardiac ion channel activity and expression.

A registry-based cohort analysis was performed in 33 consecutive patients who underwent cardiac magnetic resonance imaging for suspected ibrutinib-related cardiotoxicity. Approximately two-thirds of the patients showed signs of myocardial damage, including more than 50% with late gadolinium

enhancement fibrosis. Myocardial fibrosis was prevalent in patients with ibrutinib-related cardiotoxicity and appeared to be associated with an increased risk of cardiotoxicity [41]. In our study, ibrutinib promoted α-SMA expression, indicating cardiac fibroblast activation and differentiation to myofibroblasts, which leads to cardiac fibrosis.

In the myocardium, AKT serves as a major signal transducer, and the PI3K/AKT pathway is responsible for maintaining metabolic balance and regulating cellular responses. PI3K consists of the catalytic p110 subunit and the regulatory p85 subunit. Inactive cardiac myocyte-specific PI3K (p110α) results in delayed cardiac growth, reduced contractility, and impaired cardiopulmonary function, leading to an increased mortality risk during early life [42, 43]. AKT is an essential downstream protein of the PI3K signaling pathway, and it plays a critical role in antiapoptosis [44]. In microvascular endothelial cells, PI3K/AKT induces the expression of survivin and suppresses the activity of caspase-3 to inhibit the apoptotic effects induced by angiotensin II [32]. Metformin is an antidiabetic agent that

exerts cardioprotective effects by activating AMPK. Inhibiting AMPK phosphorylation downregulates the expression of gap junctions and ion channels, leading to abnormal conduction [45]. In this study, metformin prevented ibrutinib-induced ventricular remodeling and arrhythmia by activating the AMPK and PI3K/AKT pathway and inhibiting apoptosis of cardiomyocytes.

This study investigated the effects and mechanism by which metformin ameliorates structural ventricular remodeling and conduction abnormalities induced by ibrutinib. Metformin can ameliorate myocardial damage caused by ibrutinib through increased activation of PI3K/AKT, thereby exerting an anti-apoptotic effect. Therefore, metformin could serve as a potential therapeutic strategy to counteract the cardiotoxicity associated with ibrutinib treatment in patients with B cell cancer.

This study has some limitations. First, we investigated whether metformin ameliorates the cardiotoxicity of ibrutinib to a certain extent, but whether metformin can reverse the cardiotoxicity of ibrutinib is still unclear. Therefore, further studies on this issue are required. Second, a major limitation of basic science research in cardio-oncology is the lack of well-optimized animal models mimicking the real-world patient phenotype. The dose of metformin that we used may have been higher than current clinical use because we did not use a mouse tumor model, and this may limit the clinical applicability. Third, the dose of metformin used is not comparable to that used in clinical practice. The dosage was specifically selected to influence mitochondrial function in mice, which may restrict the clinical relevance of our findings. However, it is important to note that even a low dose of metformin can still activate AMPK, thereby initiating downstream signaling pathways [46]. Further studies are required to address this issue.

## 5 | Conclusions

This study shows that ibrutinib has detrimental effects on cardiac function, promoting ventricular arrhythmia and inducing ventricular structural remodeling. These adverse effects are associated with reduced activity of the PI3K-AKT pathway, leading to apoptosis of cardiomyocytes. However, the administration of metformin before ibrutinib treatment mitigates these cardiotoxic effects. Metformin improves ventricular arrhythmia, preserves electrical conduction, and ameliorates cardiac dysfunction and structural remodeling induced by ibrutinib. The protective effects of metformin are attributed to its ability to promote AMPK and PI3K-AKT pathway activity and modulate apoptosis of cardiomyocytes.

### Author Contributions

**Pengsha Li:** conceptualization (equal), data curation (equal), formal analysis (equal), investigation (equal), methodology (equal), project administration (equal), supervision (equal), writing – original draft (equal). **Daiqi Liu:** conceptualization (equal), formal analysis (equal), methodology (equal), project administration (equal), supervision (equal), visualization (equal), writing – review and editing (equal). **Pan Gao:** investigation (equal), software (equal), supervision (equal), validation (equal), visualization (equal), writing – review and editing (equal). **Ming**

**Yuan:** conceptualization (equal), funding acquisition (equal), methodology (equal), resources (equal). **Zhiqiang Zhao:** conceptualization (equal), methodology (equal), writing – review and editing (equal). **Yue Zhang:** conceptualization (equal), investigation (equal), methodology (equal), project administration (equal). **Zandong Zhou:** formal analysis (equal), investigation (equal), project administration (equal). **Qingling Zhang:** conceptualization (equal), investigation (equal), project administration (equal). **Meng Yuan:** conceptualization (equal), methodology (equal). **Xing Liu:** conceptualization (equal), methodology (equal). **Gary Tse:** writing – review and editing (equal). **Guangping Li:** conceptualization (equal), writing – review and editing (equal). **Qiankun Bao:** conceptualization (equal), project administration (equal), supervision (equal), writing – review and editing (equal). **Tong Liu:** funding acquisition (lead), resources (equal), writing – review and editing (equal).

### Acknowledgments

The authors have nothing to report.

### Ethics Statement

The study protocols and use of animals were approved by the Experimental Animal Administration Committee of Tianjin Medical University (TMUAMEC 2019004).

### Consent

The authors have nothing to report.

### Conflicts of Interest

Professor Tong Liu is the member of the *Cancer Innovation* Editorial Board. To minimize bias, he was excluded from all editorial decision-making related to the acceptance of this article for publication. The remaining authors declare no conflicts of interest.

### Data Availability Statement

The analyzed data sets generated during the present study are available from the corresponding author upon reasonable request.

### References

1. X. Yang, N. An, C. Zhong, et al., “Enhanced Cardiomyocyte Reactive Oxygen Species Signaling Promotes Ibrutinib-Induced Atrial Fibrillation,” *Redox Biology* 30 (2020): 101432, <https://doi.org/10.1016/j.redox.2020.101432>.
2. Z. Pan, H. Scheerens, S. J. Li, et al., “Discovery of Selective Irreversible Inhibitors for Bruton's Tyrosine Kinase,” *Chem Med Chem* 2, no. 1 (2007): 58–61, <https://doi.org/10.1002/cmdc.200600221>.
3. S. K. Gülsaran, M. Baysal, U. Demirci, et al., “Late Onset Left Ventricular Dysfunction and Cardiomyopathy Induced With Ibrutinib,” *Journal of Oncology Pharmacy Practice* 26, no. 2 (2020): 478–480, <https://doi.org/10.1177/1078155219852146>.
4. J. C. Byrd, R. R. Furman, S. E. Coutre, et al., “Three-Year Follow-Up of Treatment-Naïve and Previously Treated Patients With CLL and SLL Receiving Single-Agent Ibrutinib,” *Blood* 125, no. 16 (2015): 2497–2506, <https://doi.org/10.1182/blood-2014-10-606038>.
5. M. Sestier, C. Hillis, G. Fraser, and D. Leong, “Bruton's Tyrosine Kinase Inhibitors and Cardiotoxicity: More Than Just Atrial Fibrillation,” *Current Oncology Reports* 23, no. 10 (2021): 113, <https://doi.org/10.1007/s11912-021-01102-1>.
6. S. Yun, N. D. Vincelette, U. Acharya, and I. Abraham, “Risk of Atrial Fibrillation and Bleeding Diathesis Associated With Ibrutinib Treatment: A Systematic Review and Pooled Analysis of Four Randomized Controlled Trials,” *Clinical Lymphoma Myeloma and Leukemia* 17, no. 1 (2017): 31–37.e13, <https://doi.org/10.1016/j.clml.2016.09.010>.

7. B. L. Lampson, L. Yu, R. J. Glynn, et al., "Ventricular Arrhythmias and Sudden Death in Patients Taking Ibrutinib," *Blood* 129, no. 18 (2017): 2581–2584, <https://doi.org/10.1182/blood-2016-10-742437>.
8. J. E. Salem, A. Manouchehri, M. Bretagne, et al., "Cardiovascular Toxicities Associated With Ibrutinib," *Journal of the American College of Cardiology* 74, no. 13 (2019): 1667–1678, <https://doi.org/10.1016/j.jacc.2019.07.056>.
9. J. Tomcsányi, Z. Nényei, Z. Mátrai, and B. Bózsik, "Ibrutinib, an Approved Tyrosine Kinase Inhibitor as a Potential Cause of Recurrent Polymorphic Ventricular Tachycardia," *JACC: Clinical Electrophysiology* 2, no. 7 (2016): 847–849, <https://doi.org/10.1016/j.jacep.2016.07.004>.
10. R. Dong, Y. Yan, X. Zeng, N. Lin, and B. Tan, "Ibrutinib-Associated Cardiotoxicity: From the Pharmaceutical to the Clinical," *Drug Design, Development and Therapy* 16 (2022): 3225–3239, <https://doi.org/10.2147/DDDT.S377697>.
11. R. W. Hendriks, S. Yuvaraj, and L. P. Kil, "Targeting Bruton's Tyrosine Kinase in B Cell Malignancies," *Nature Reviews Cancer* 14, no. 4 (2014): 219–232, <https://doi.org/10.1038/nrc3702>.
12. L. Pretorius, X. J. Du, E. A. Woodcock, et al., "Reduced Phosphoinositide 3-Kinase (p110 $\alpha$ ) Activation Increases the Susceptibility to Atrial Fibrillation," *American Journal of Pathology* 175, no. 3 (2009): 998–1009, <https://doi.org/10.2353/ajpath.2009.090126>.
13. J. R. McMullen, E. J. H. Boey, J. Y. Y. Ooi, J. F. Seymour, M. J. Keating, and C. S. Tam, "Ibrutinib Increases the Risk of Atrial Fibrillation, Potentially Through Inhibition of Cardiac PI3K-Akt Signaling," *Blood* 124, no. 25 (2014): 3829–3830, <https://doi.org/10.1182/blood-2014-10-604272>.
14. F. Han, C. F. Li, Z. Cai, et al., "The Critical Role of AMPK in Driving Akt Activation Under Stress, Tumorigenesis and Drug Resistance," *Nature Communications* 9, no. 1 (2018): 4728, <https://doi.org/10.1038/s41467-018-07188-9>.
15. C. Snehalatha, S. Priscilla, A. Nanditha, R. Arun, K. Satheesh, and A. Ramachandran, "Metformin in Prevention of Type 2 Diabetes," *Journal of the Association of Physicians of India* 66, no. 3 (2018): 60–63.
16. M. Foretz, B. Guigas, and B. Viollet, "Understanding the Glucoregulatory Mechanisms of Metformin in Type 2 Diabetes Mellitus," *Nature Reviews Endocrinology* 15, no. 10 (2019): 569–589, <https://doi.org/10.1038/s41574-019-0242-2>.
17. H. Loi, F. Boal, H. Tronchere, et al., "Metformin Protects the Heart against Hypertrophic and Apoptotic Remodeling After Myocardial Infarction," *Frontiers in Pharmacology* 10 (2019): 154, <https://doi.org/10.3389/fphar.2019.00154>.
18. D. M. Charytan, S. D. Solomon, P. Ivanovich, et al., "Metformin use and Cardiovascular Events in Patients With Type 2 Diabetes and Chronic Kidney Disease," *Diabetes, Obesity and Metabolism* 21, no. 5 (2019): 1199–1208, <https://doi.org/10.1111/dom.13642>.
19. G. Rena and C. C. Lang, "Repurposing Metformin for Cardiovascular Disease," *Circulation* 137, no. 5 (2018): 422–424, <https://doi.org/10.1161/CIRCULATIONAHA.117.031735>.
20. S. Gundewar, J. W. Calvert, S. Jha, et al., "Activation of AMP-Activated Protein Kinase by Metformin Improves Left Ventricular Function and Survival in Heart Failure," *Circulation Research* 104, no. 3 (2009): 403–411, <https://doi.org/10.1161/CIRCRESAHA.108.190918>.
21. K. Færch, H. Amadid, L. B. Nielsen, et al., "Protocol for a Randomised Controlled Trial of the Effect of Dapagliflozin, Metformin and Exercise on Glycaemic Variability, Body Composition and Cardiovascular Risk in Prediabetes (The PRE-D Trial)," *BMJ Open* 7, no. 5 (2017): e013802, <https://doi.org/10.1136/bmjopen-2016-013802>.
22. R. Wurm, M. Resl, S. Neuhold, et al., "Cardiovascular Safety of Metformin and Sulfonylureas in Patients With Different Cardiac Risk Profiles," *Heart* 102, no. 19 (2016): 1544–1551, <https://doi.org/10.1136/heartjnl-2015-308711>.
23. T. Takiuchi, H. Machida, M. S. Hom, et al., "Association of Metformin use and Survival Outcome in Women With Cervical Cancer," *International Journal of Gynecological Cancer* 27, no. 7 (2017): 1455–1463, <https://doi.org/10.1097/IGC.0000000000001036>.
24. N. Saini and X. Yang, "Metformin as an Anti-Cancer Agent: Actions and Mechanisms Targeting Cancer Stem Cells," *Acta biochimica et biophysica Sinica* 50, no. 2 (2018): 133–143, <https://doi.org/10.1093/abbs/gmx106>.
25. C. Xia, R. Chen, J. Chen, et al., "Combining Metformin and Nelfinavir Exhibits Synergistic Effects Against the Growth of Human Cervical Cancer Cells and Xenograft in Nude Mice," *Scientific Reports* 7 (2017): 43373, <https://doi.org/10.1038/srep43373>.
26. Z. Xie, K. Lau, B. Eby, et al., "Improvement of Cardiac Functions by Chronic Metformin Treatment Is Associated With Enhanced Cardiac Autophagy in Diabetic OVE26 Mice," *Diabetes* 60, no. 6 (2011): 1770–1778, <https://doi.org/10.2337/db10-0351>.
27. N. Li and X. H. Wehrens, "Programmed Electrical Stimulation in Mice," *JoVE: Journal of Visualized Experiments*, no. 39 (2010): 1730, <https://doi.org/10.3791/1730>.
28. S. Petric, L. Clasen, C. van Weßel, et al., "In Vivo Electrophysiological Characterization of TASK-1 Deficient Mice," *Cellular Physiology and Biochemistry* 30, no. 3 (2012): 523–537, <https://doi.org/10.1159/000341435>.
29. M. B. Thomsen, M. S. Nielsen, A. Aarup, L. S. Bisgaard, and T. X. Pedersen, "Uremia Increases Qrs Duration After  $\beta$ -adrenergic Stimulation in Mice," *Physiological Reports* 6, no. 13 (2018): e13720, <https://doi.org/10.14814/phy2.13720>.
30. M. Gong, M. Yuan, L. Meng, et al., "Wenxin Keli Regulates Mitochondrial Oxidative Stress and Homeostasis and Improves Atrial Remodeling in Diabetic Rats," *Oxidative Medicine and Cellular Longevity* 2020 (2020): 1–17, <https://doi.org/10.1155/2020/2468031>.
31. S. Ning, S. Zhang, and Z. Guo, "MicroRNA-494 Regulates High Glucose-Induced Cardiomyocyte Apoptosis and Autophagy by PI3K/AKT/mTOR Signalling Pathway," *ESC Heart Failure* 10, no. 2 (2023): 1401–1411, <https://doi.org/10.1002/ehf2.14311>.
32. H. Ohashi, H. Takagi, H. Oh, et al., "Phosphatidylinositol 3-kinase/Akt Regulates Angiotensin II-Induced Inhibition of Apoptosis in Microvascular Endothelial Cells by Governing Survivin Expression and Suppression of Caspase-3 Activity," *Circulation Research* 94, no. 6 (2004): 785–793, <https://doi.org/10.1161/01.RES.0000121103.03275.EC>.
33. A. R. Cameron, V. L. Morrison, D. Levin, et al., "Anti-Inflammatory Effects of Metformin Irrespective of Diabetes Status," *Circulation Research* 119, no. 5 (2016): 652–665, <https://doi.org/10.1161/CIRCRESAHA.116.308445>.
34. J. M. M. Evans, S. A. Ogston, A. Emslie-Smith, and A. D. Morris, "Risk of Mortality and Adverse Cardiovascular Outcomes in Type 2 Diabetes: A Comparison of Patients Treated With Sulfonylureas and Metformin," *Diabetologia* 49, no. 5 (2006): 930–936, <https://doi.org/10.1007/s00125-006-0176-9>.
35. F. A. Duca, C. D. Côté, B. A. Rasmussen, et al., "Metformin Activates a Duodenal AMPK-Dependent Pathway to Lower Hepatic Glucose Production in Rats," *Nature Medicine* 21, no. 5 (2015): 506–511, <https://doi.org/10.1038/nm.3787>.
36. A. Guha, M. H. Derbala, Q. Zhao, et al., "Ventricular Arrhythmias Following Ibrutinib Initiation for Lymphoid Malignancies," *Journal of the American College of Cardiology* 72, no. 6 (2018): 697–698, <https://doi.org/10.1016/j.jacc.2018.06.002>.
37. S. Bravaccini, G. Martinelli, and C. Cerchione, "What Influences the Choice of Ibrutinib-Rituximab Vs Classic Chemoimmunotherapy for Chronic Lymphocytic Leukemia?," *Cell Transplantation* 29 (2020): 096368972095020, <https://doi.org/10.1177/0963689720950209>.

38. B. W. Christensen, V. G. Zaha, and F. T. Awan, "Cardiotoxicity of BTK Inhibitors: Ibrutinib and Beyond," *Expert Review of Hematology* 15, no. 4 (2022): 321–331, <https://doi.org/10.1080/17474086.2022.2067526>.
39. J. Alexandre, J. J. Moslehi, K. R. Bersell, C. Funck-Brentano, D. M. Roden, and J. E. Salem, "Anticancer Drug-Induced Cardiac Rhythm Disorders: Current Knowledge and Basic Underlying Mechanisms," *Pharmacology & Therapeutics* 189 (2018): 89–103, <https://doi.org/10.1016/j.pharmthera.2018.04.009>.
40. R. R. Shah and J. Morganroth, "Update on Cardiovascular Safety of Tyrosine Kinase Inhibitors: With a Special Focus on QT Interval, Left Ventricular Dysfunction and Overall Risk/Benefit," *Drug Safety* 38, no. 8 (2015): 693–710, <https://doi.org/10.1007/s40264-015-0300-1>.
41. B. Buck, A. P. Chum, M. Patel, et al., "Cardiovascular Magnetic Resonance Imaging in Patients With Ibrutinib-Associated Cardiotoxicity," *JAMA Oncology* 9, no. 4 (2023): 552–555, <https://doi.org/10.1001/jamaoncol.2022.6869>.
42. M. Abdellatif, V. Trummer-Herbst, A. M. Heberle, et al., "Fine-Tuning Cardiac Insulin-Like Growth Factor 1 Receptor Signaling to Promote Health and Longevity," *Circulation* 145, no. 25 (2022): 1853–1866, <https://doi.org/10.1161/CIRCULATIONAHA.122.059863>.
43. M. Abdellatif, T. Eisenberg, A. M. Heberle, K. Thedieck, G. Kroemer, and S. Sedej, "Cardiac PI3K p110 $\alpha$  Attenuation Delays Aging and Extends Lifespan," *Cell Stress* 6, no. 8 (2022): 72–75, <https://doi.org/10.15698/cst2022.08.270>.
44. R. Aikawa, M. Nawano, Y. Gu, et al., "Insulin Prevents Cardiomyocytes From Oxidative Stress-Induced Apoptosis Through Activation of Pi<sub>3</sub> kinase/Akt," *Circulation* 102, no. 23 (2000): 2873–2879, <https://doi.org/10.1161/01.cir.102.23.2873>.
45. L. Wang, X. Li, Z. Yang, et al., "Crotonaldehyde Induces Autophagy-Mediated Cytotoxicity in Human Bronchial Epithelial Cells via PI3K, AMPK and MAPK pathways," *Environmental Pollution* 228 (2017): 287–296, <https://doi.org/10.1016/j.envpol.2017.03.083>.
46. T. Ma, X. Tian, B. Zhang, et al., "Low-Dose Metformin Targets the Lysosomal AMPK Pathway Through Pen2," *Nature* 603, no. 7899 (2022): 159–165, <https://doi.org/10.1038/s41586-022-04431-8>.